

Local Electronic Properties of Titanocene Chloride Dimer Molecules on a Metal Surface

Ryan Yamachika,[†] Xinghua Lu,^{†,‡} Daniel Wegner,[†] Yayu Wang,[†] Andre Wachowiak,^{†,‡} Michael Grobis,[†] Lianne M. C. Beltran,[§] Jeffrey R. Long,[§] Mark Pederson,^{||} and Michael F. Crommie^{*,†,‡}

Department of Physics, University of California, Berkeley, Berkeley, California 94720, Materials Sciences Division, Lawrence Berkeley National Laboratory, Berkeley, California 94720, Department of Chemistry, University of California, Berkeley, Berkeley, California 94720, and USN, Research Laboratory, Center for Computational Materials Science, Code 6392, Washington, D.C. 20375

Received: August 27, 2008; Revised Manuscript Received: October 11, 2008

We have examined the local electronic behavior of titanocene chloride dimer molecules, $[\text{Cp}_2\text{TiCl}]_2$ ($\text{Cp} = \text{C}_5\text{H}_5$), on Au(111) using both scanning tunneling microscopy (STM) and density functional theory (DFT). Isolated dimeric molecules are seen to decorate gold step edges at low surface coverages and two coexisting monolayer phases are observed at higher coverages. Differential conductance STM spectroscopy shows a variety of structure in the electronic local density of states for single molecules and for the two monolayer phases. DFT calculations modeling an isolated titanocene chloride dimer do not reproduce the wide variations seen in spectral density, suggesting that a fraction of titanocene dimers break apart into metallocene monomers on the Au(111) surface and display magnetic behavior.

Introduction

The titanocene chloride dimer (Figure 1a) is known for its utility as an inexpensive reducing agent in organic synthesis, as well as for its magnetic properties. It catalyzes radical ring opening in epoxides,¹ as well as reduction and pinacol coupling of carbonyls,² and can be used as a single electron transfer agent.^{3,4} Antiferromagnetic coupling between the spins of the two titanium atoms in this molecule makes it a candidate for studying magnetism at nanometer length scales.⁵ Many potential nanotechnological applications of this molecule, such as in single molecule transistors, involve tethering it to conducting surfaces, which requires precise control of molecule-surface chemistry.^{6–8} Currently, however, the influence of metal substrates on the adsorption, catalytic, and magnetic properties of titanocene chloride dimers is unknown, and previous studies on other molecules have shown that this is an important topic to understand.^{9–11}

To investigate the impact of a metal substrate on the behavior of titanocene chloride dimers, we used a combination of scanning tunneling microscopy (STM) and density functional theory (DFT) methods to study the titanocene chloride dimer molecules deposited onto the surface of Au(111). Our STM topographs reveal isolated dimer molecules at gold step edges for low molecular coverages, as well as two different coexisting phases at higher coverages closer to a monolayer. The electronic structure of both the isolated molecules and the higher coverage monolayer phases were experimentally studied via STM differential conductance (dI/dV) spectroscopy. Large reproducible variations in dI/dV spectra were observed between the different molecular morphologies. To explain this behavior, the density of electronic states (DOS) of an isolated titanocene chloride

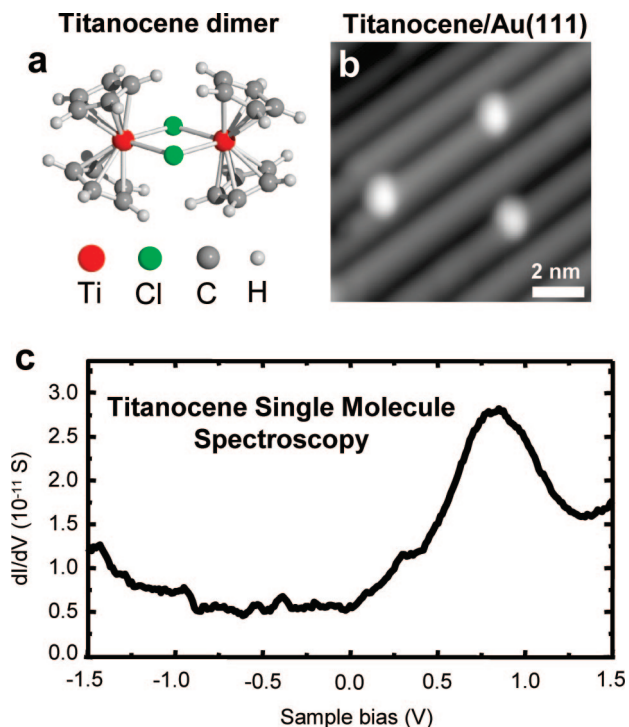


Figure 1. (a) DFT calculated structural model of the free titanocene chloride dimer. (b) STM topograph taken at $V = 1.0$ V, $I = 20$ pA of isolated molecules at step edges of Au(111) ($T = 7$ K). The terrace width here is about 2 nm. (c) dI/dV spectroscopy of single molecules shows a LUMO resonance around 0.8 V. This spectrum is an average of spectra taken over many molecules.

* Corresponding author. Phone: (510) 642-9392. Fax: (510) 642-9398. E-mail: crommie@berkeley.edu.

[†] Department of Physics, University of California.

[‡] Materials Sciences Division, Lawrence Berkeley National Laboratory.

[§] Department of Chemistry, University of California.

^{||} USN, Research Laboratory, Center for Computational Materials Science.

dimer was calculated by using DFT. The calculated properties of a dimer, however, do not account for all of our observed spectroscopic features. We find that the additional observed spectral features (which include a spin-induced Kondo resonance) can be explained by the coexistence of Cp_2Ti and

Cp_2TiCl_2 monomers in one of the monolayer phases, suggesting that a fraction of titanocene chloride dimers split into monomers on Au(111).

Experimental Methods

Our experiments were conducted with a home-built ultrahigh vacuum (UHV) STM with a PtIr tip operated at 7 K. Titanocene chloride was synthesized by using the second method provided by Green and Lucas.¹² The material was then further purified by sublimation. The single-crystal Au(111) substrate was cleaned in UHV prior to deposition of titanocene chloride dimers from a Knudsen cell at 85 °C onto a room temperature substrate. The dI/dV spectra were measured through lock-in detection of the ac tunneling current driven by a 451 Hz, 1–10 mV (rms) signal added to the junction bias under open-loop conditions (bias voltage here is defined as the sample potential referenced to the tip).

Results and Discussion

Isolated titanocene chloride dimer molecules on Au(111) step edges are seen in the STM topograph in Figure 1b. Individual molecules appear as slightly asymmetrical protrusions with a height of 2.2 Å, as measured at 1.0 V sample bias and 20 pA tunneling current. There is no discernible variation in the shape of the molecule when imaged at different biases in a ± 1.5 V window. The exact orientation of the molecule on the surface cannot be determined from STM topographs, but little variation was observed between different isolated molecules. The dI/dV spectrum (Figure 1c) clearly shows a lowest unoccupied molecular orbital (LUMO) resonance around 0.8 V.

At higher molecular coverages (greater than 10% of a monolayer), two new phases were discovered to coexist, here referred to as phase 1 and phase 2 (Figure 2a). High-resolution topographs of phase 1 (Figure 2b) reveal a periodic network of protrusions having varying shapes and heights. Dim protrusions in this phase appear elongated while brighter protrusions are circular (seven dim protrusions surround each bright one). The morphology of phase 2 is quite different, as the shapes of all protrusions here appear more circular, and the molecular arrangement has a honeycomb-like structure (every phase 2 bright protrusion is surrounded by three bright and three dim protrusions). Notice that the size of the protrusions seen in phase 2 is different from that seen in phase 1 and single molecules. This likely arises from a combination of effects, including molecular orientation, electronic structure, and STM tip size. Attempts to match the experimentally observed two-dimensional structures to surface terminations of known bulk geometries of $[\text{Cp}_2\text{TiCl}]_2$ were unsuccessful,^{5,13,14} implying that a new 2-D molecular ordering occurs at the surface of gold.

The local electronic structure of phase 1 and phase 2 monolayers was measured by using STM dI/dV spectroscopy. The dI/dV spectrum of phase 1 (Figure 3a) reveals multiple peaks with amplitudes that depend on where the spectrum is taken spatially. The brighter phase 1 protrusions (circled in red Figure 3b) show a LUMO at about 0.5 V and a highest occupied molecular orbital (HOMO) at about -1.0 V, while the dimmer regions (circled in green) show only one distinct resonance at around 1.3 V. Spectroscopy at higher voltages was not possible since it caused irreversible damage to the monolayer structure.

Local dI/dV spectroscopy performed in phase 2 regions (Figure 4a) shows resonant peaks at different energies than those seen in phase 1. The brighter protrusions (circled in red in Figure 4b) display a pronounced peak at -0.3 V. The dimmer regions (circled in green) display electronic resonances at -1.1 and 0.3

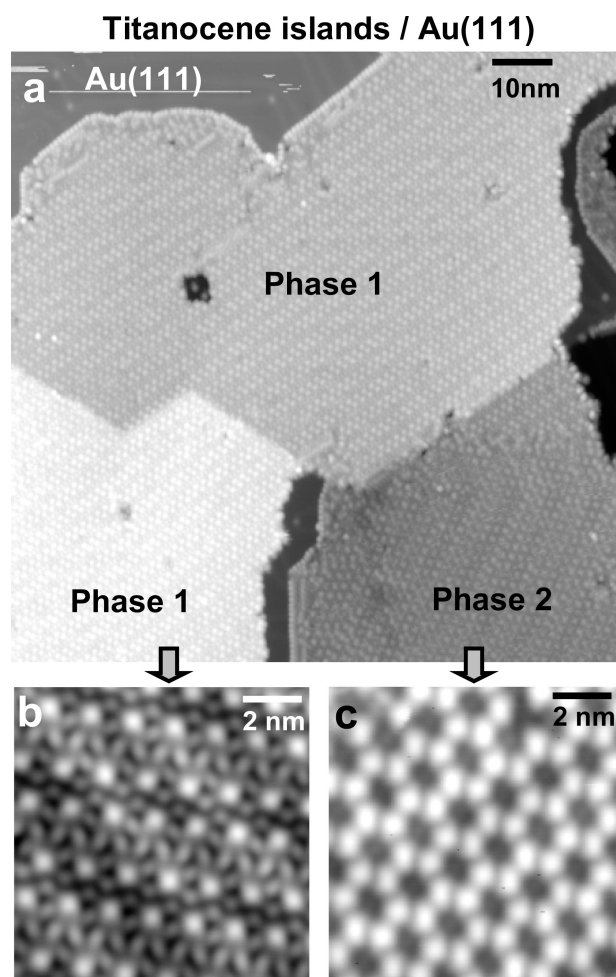


Figure 2. (a) STM topograph taken at $V = 1.0$ V and $I = 5$ pA showing the coexistence of both phase 1 and phase 2 titanocene monolayers with regions of clean Au(111) ($T = 7$ K). The terraces here are approximately 150 nm wide. (b) High-resolution STM topograph of phase 1 ($V = -1.0$ V, $I = 10$ pA). (c) High-resolution topograph of phase 2 ($V = -0.5$ V, $I = 5$ pA).

V. The spectrum in the dimmer region cuts off at 0.3 V since the dI/dV signal gets very noisy for larger biases. At higher energy resolution, a Kondo peak can be seen at $V = 0$ in the dim regions of phase 2 (Figure 4a, inset). Such a peak is never seen in phase 1. Fitting the Kondo resonance to a Fano line shape after thermal deconvolution¹⁵ yields a line width of $\Gamma = 8.6$ meV, from which a Kondo temperature of $T = 50$ K is derived.¹⁶

To understand the wide range of behavior observed in our experimental spectra, we performed first-principles DFT calculations on free titanocene chloride dimers using the NRLMOL code.^{17,18} Effects of the surface can be important, but were not included since we do not know the exact molecular arrangement (there are many possibilities) and performing a calculation for every possible arrangement is prohibitively expensive. However, we still expect the free molecule calculations to give a qualitative understanding of the experimental data. All atoms in the calculation were treated within an all-electron approach.¹⁷ The basis sets used in these calculations are roughly equivalent to triple- ζ or better.¹⁹ The generalized gradient approximation (PBE-GGA) was used to approximate the exchange-correlation functional.²⁰ Free molecules were relaxed until all forces were below 0.01 eV/Å.

The ground state of $[\text{Cp}_2\text{TiCl}]_2$ is found to have antiferromagnetic coupling between the two Ti(III) atoms' spins with a

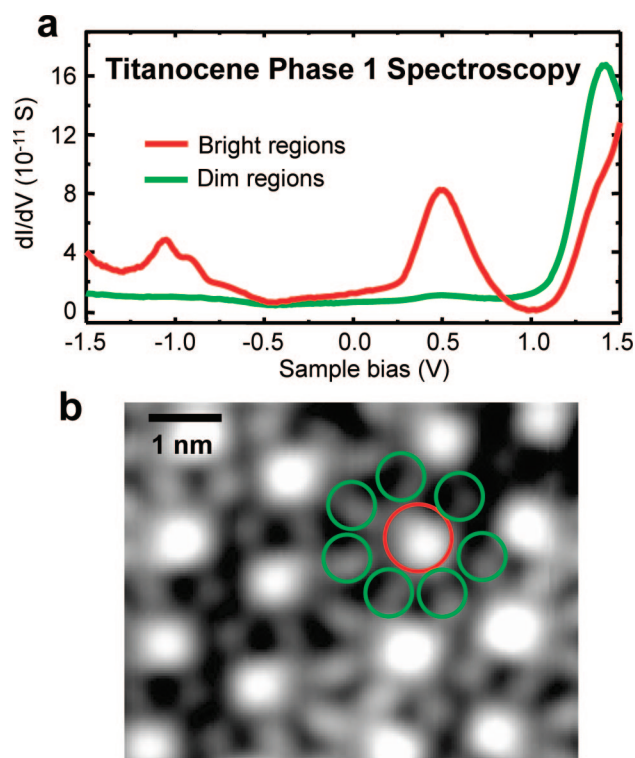


Figure 3. Spatially dependent dI/dV spectroscopy of phase 1 ($T = 7$ K). (a) The green curve is the spatial average of spectra taken at different points within the dim phase 1 regions, while the red curve is the spatial average of spectra taken at different points within the brighter regions. (b) STM topograph of phase 1 ($V = -1.5$ V, $I = 10$ pA) showing dim regions circled in green and brighter regions circled in red.

singlet-to-triplet transition energy of 13.3 meV, consistent with previous bulk measurements.⁵ Figure 5a (lower panel) shows the DOS calculated for a free titanocene chloride dimer. The graph has been rigidly shifted within the HOMO/LUMO gap to align the energetic positions of the theoretical HOMO/LUMO peaks with our experimental spectra since the precise location of the Fermi energy is not well defined for a free molecule with a wide HOMO/LUMO gap. As seen in Figure 5a (top panel) the calculated peaks line up reasonably well with the experimental spectra both for isolated dimer molecules as well as for phase 1 bright and dim molecular features. Differences in experimental peak positions and magnitudes between the isolated and phase 1 molecules are likely due to differing molecular orientations on the surface. The specific orientations are difficult to determine due to the wide number of possible structures that could potentially fit our data. The electronic structure seen in the experimental spectra for phase 2 molecules shows a dramatic departure from the isolated molecule and phase 1 behavior, which our DFT dimer calculations do not account for. We also note that the phase 2 topographic molecular features are more circular in comparison to the elongated features of phase 1 molecules. As a result of these differences between phase 1 and phase 2, we propose that phase 2 is composed of an array of titanocene monomers. Molecular dissociation may happen during the thermal evaporation process, or may occur on the surface, which is known to occur for other metallocenes.²¹ A well-known stable fragment of the titanocene chloride dimer is titanocene dichloride (Cp_2TiCl_2). The presence of this monomer on the Au(111) surface suggests (stoichiometrically) the simultaneous existence of the nonchlorinated titanocene monomer (Cp_2Ti).

This interpretation is supported by comparisons of our measured dI/dV spectra with DFT calculations of the DOS of

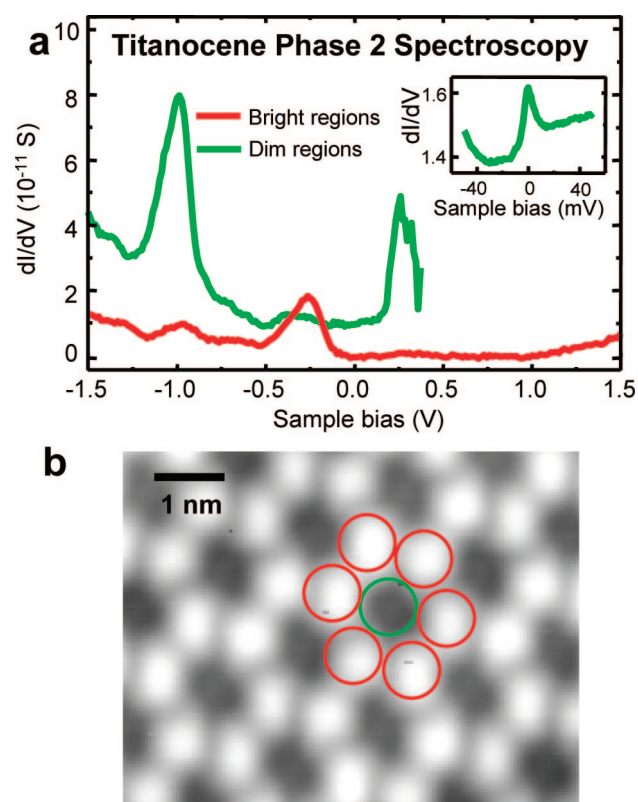


Figure 4. Spatially dependent dI/dV spectroscopy of phase 2 ($T = 7$ K). (a) The green curve is the spatial average of spectra taken at different points within the dim phase 2 regions, while the red curve is the spatial average of spectra taken at different points within the brighter regions. The inset shows a Kondo peak observed only in the phase 2 dim regions. (b) STM topograph of phase 2 ($V = -0.5$ V, $I = 5$ pA) showing the dim regions circled in green and brighter regions circled in red.

Cp_2TiCl_2 and Cp_2Ti . The lower panel of Figure 5b shows the calculated DOS (broken down by element) for both free Cp_2TiCl_2 and Cp_2Ti monomers (these results are also consistent with previous total DOS calculations^{22,23}). The free-molecule Fermi level of Cp_2TiCl_2 is not well-defined due to its wide HOMO/LUMO gap, and so its theoretical spectrum has been rigidly shifted within the HOMO/LUMO gap to line up the calculated peaks with experimental features. The free molecule Cp_2Ti spectrum, on the other hand, has a more well-defined Fermi level since the HOMO/LUMO gap here is so small, and so its energy alignment is pinned. Both types of monomers are seen to have new states near E_F that do not exist in the dimer calculations, consistent with experiment and thus supporting the proposal that phase 2 consists of titanocene monomers instead of dimers. The calculated Cp_2TiCl_2 spectrum, for example, has filled states similar to features seen in the experimental spectra for phase 2 bright regions (Figure 5b, top panel) while the calculated spectrum for Cp_2Ti has unoccupied states near E_F , similar to the dim regions of phase 2. This suggests that the bright regions in phase 2 are Cp_2TiCl_2 monomers while the dim regions are Cp_2Ti monomers. The experimentally observed Kondo peak in the phase 2 dim regions is consistent with magnetism predicted in our calculations for Cp_2Ti ($S = 1$), while the lack of a Kondo peak in phase 2 bright regions is consistent with the nonmagnetic $S = 0$ ground state of Cp_2TiCl_2 seen in our calculations.²³ The exact molecular orientations and adsorption sites of the two monomers in this phase could not be precisely determined for the same reasons stated above regarding phase 1. We also note that the experimental ratio of Cp_2Ti to Cp_2TiCl_2 is 1:2, which deviates from the expected 1:1 ratio,

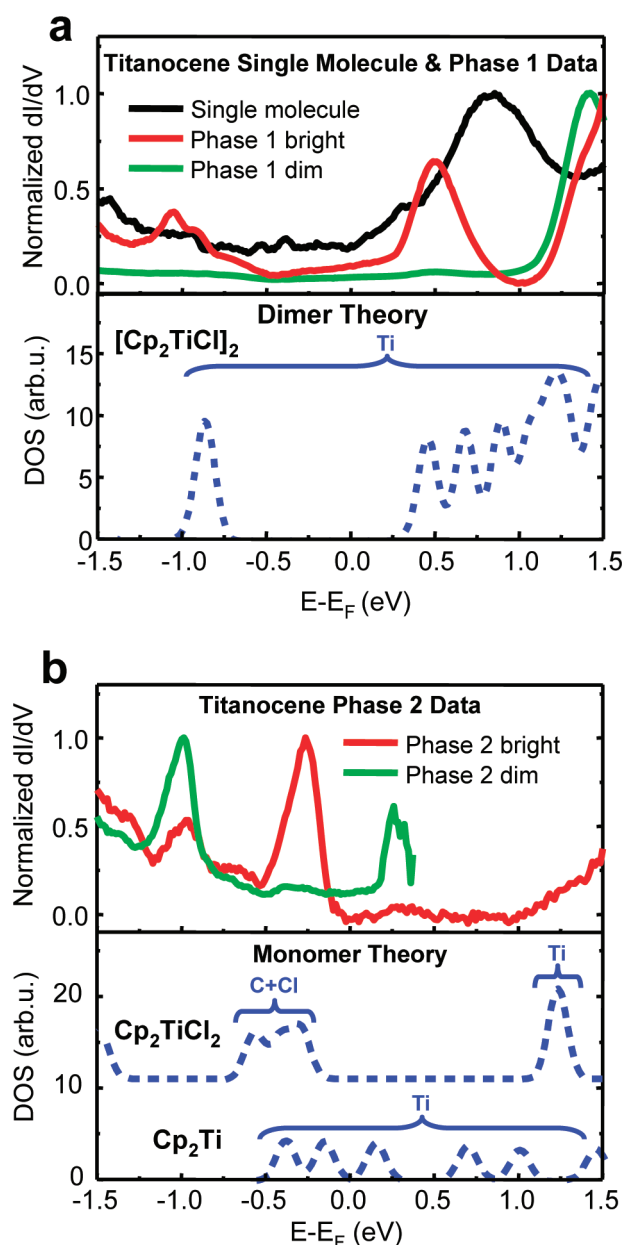


Figure 5. Comparison of experimental spectra to theoretical DOS. (a) The upper panel shows experimental dI/dV spectra for isolated molecules and the phase 1 monolayer of titanocene chloride dimers on Au(111) (each spectrum has been normalized by its highest amplitude point). The lower panel shows the broadened theoretical DOS (including elemental breakdown) for a free titanocene chloride dimer. (b) The upper panel shows experimental dI/dV spectra for the phase 2 monolayer where each spectrum has been normalized by its highest amplitude point. The lower panel shows the broadened calculated DOS (including elemental breakdown) for the two monomer species Cp_2TiCl_2 and Cp_2Ti as free molecules, vertically shifted for clarity.

possibly due to a smaller sticking probability for Cp_2Ti that causes a fraction of them to desorb from the Au(111) surface.

Conclusions

In conclusion, we have studied the behavior of titanocene chloride dimers at a noble metal surface using STM and DFT calculations. Isolated molecules and two new monolayer phases were experimentally observed on the Au(111) surface. Our DFT calculations of free molecules suggest that full dimers, as well as two different monomer species, Cp_2TiCl_2 (nonmagnetic) and Cp_2Ti (magnetic), coexist on Au(111). We expect that the molecular adsorption geometries could be better determined, and the agreement between experimental spectroscopy and theory improved, if further effects of the surface (such as surface hybridization, relaxation, and charge transfer) and overlap between tip and molecule wave functions were included in future calculations.

Acknowledgment. This work was supported by NSF Grant ECS-0609469. D.W. is grateful for funding by the Alexander von Humboldt Foundation. Y.W. thanks the Miller Institute for a research fellowship.

References and Notes

- (1) Rajanbabu, T. V.; Nugent, W. A. *J. Am. Chem. Soc.* **1994**, *116*, 986–997.
- (2) Gansauer, A. *Chem. Commun.* **1997**, 457–458.
- (3) Barden, M. C.; Schwartz, J. J. *Am. Chem. Soc.* **1996**, *118*, 5484–5485.
- (4) Asandei, A. D.; Chen, Y. H. *Macromolecules* **2006**, *39*, 7549–7554.
- (5) Jungst, R.; Sekutowski, D.; Davis, J.; Luly, M.; Stucky, G. *Inorg. Chem.* **1977**, *16*, 1645–1655.
- (6) Park, J.; Pasupathy, A. N.; Goldsmith, J. I.; Chang, C.; Yaish, Y.; Petta, J. R.; Rinkoski, M.; Sethna, J. P.; Abruna, H. D.; McEuen, P. L.; Ralph, D. C. *Nature* **2002**, *417*, 722–725.
- (7) Liang, W. J.; Shores, M. P.; Bockrath, M.; Long, J. R.; Park, H. *Nature* **2002**, *417*, 725–729.
- (8) Thomas, J. M.; Raja, R. *J. Organomet. Chem.* **2004**, *689*, 4110–4124.
- (9) Hipps, K. W.; Barlow, D. E.; Mazur, U. *J. Phys. Chem. B* **2000**, *104*, 2444–2447.
- (10) Mazur, U.; Leonetti, M.; English, W. A.; Hipps, K. W. *J. Phys. Chem. B* **2004**, *108*, 17003–17006.
- (11) Barlow, D. E.; Scudiero, L.; Hipps, K. W. *Langmuir* **2004**, *20*, 4413–4421.
- (12) Green, M. L. H.; Lucas, C. R. *J. Chem. Soc., Dalton Trans.* **1972**, 1000.
- (13) Belskii, V. K.; Sokolova, I. V.; Bulychev, B. M.; Sizov, A. I. *J. Struct. Chem.* **1987**, *28*, 328–329.
- (14) Lacroix, F.; Plecnik, C. E.; Liu, S. M.; Liu, F. C.; Meyers, E. A.; Shore, S. G. *J. Organomet. Chem.* **2003**, *687*, 69–77.
- (15) Nagaoka, K.; Jamneala, T.; Grobis, M.; Crommie, M. F. *Phys. Rev. Lett.* **2002**, *88*, 077205.
- (16) Hewson, A. C. *The Kondo Problem to Heavy Fermions*; Cambridge University Press: Cambridge, UK, 1993.
- (17) Pederson, M. R.; Porezag, D. V.; Kortus, J.; Patton, D. C. *Phys. Status Solidi B* **2000**, *217*, 197–218.
- (18) Porezag, D.; Pederson, M. R.; Liu, A. Y. *Phys. Rev. B* **1999**, *60*, 14132–14139.
- (19) Porezag, D.; Pederson, M. R. *Phys. Rev. A* **1999**, *60*, 2840–2847.
- (20) Perdew, J. P.; Burke, K.; Ernzerhof, M. *Phys. Rev. Lett.* **1996**, *77*, 3865–3868.
- (21) Braun, K. F.; Iancu, V.; Pertaya, N.; Rieder, K. H.; Hla, S. W. *Phys. Rev. Lett.* **2006**, *96*, 246102.
- (22) Wang, X. J.; Chen, L.; Endou, A.; Kubo, M.; Miyamoto, A. *J. Organomet. Chem.* **2003**, *678*, 156–165.
- (23) Freitag, M. A.; Gordon, M. S. *J. Phys. Chem. A* **2002**, *106*, 7921–7926.

JP807626W